HHS Public Access

Author manuscript

J Orthop Res. Author manuscript; available in PMC 2017 June 01.

Published in final edited form as:

J Orthop Res. 2016 June ; 34(6): 1019–1025. doi:10.1002/jor.23109.

Changes in Microgaps, Micromotion and Trabecular Strain from Interlocked Cement-Trabecular Bone Interfaces in Total Knee Replacements with *In vivo* Service

Mark A. Miller[1], **Jacklyn R. Goodheart**[1], **Benjamin Khechen**[1], **Dennis Janssen**[2], and **Kenneth A. Mann**[1]

[1]Department of Orthopedic Surgery, State University of New York, Upstate Medical University, 3216 IHP, 750 East Adams Street, Syracuse, New York, 13210, USA [2]Radboud University, Nijmegen Medical Centre, Nijmegen, The Netherlands

Abstract

The initial fixation of cemented Total Knee Replacements (TKRs) relies on mechanical interlock between cement and bone, but loss of interlock occurs with *in vivo* service. In this study, cement-trabeculae gap morphology and micromechanics were measured for lab prepared (representing post-operative state) and postmortem retrieval (with *in vivo* remodeling) TKRs to determine how changes in fixation affect local micromechanics. Small specimens taken from beneath the tibial tray were loaded with 1 MPa axial compression and the local micromechanics of the trabeculae-cement interface was quantified using digital image correlation. Lab prepared trabeculae that initially interlock with cement had small gaps (ave:14μm) and limited micromotion (ave:1μm) which were larger near the cement border. Trabecular resorption was prevalent following *in vivo* service; interface gaps became larger (ave:40μm) and micromotion increased (ave:6μm), particularly near the cement border. Interlocked trabeculae from lab prepared specimens exhibited strains that were 20% of the supporting bone strain, indicating the trabeculae were initially strain shielded. The spatial and temporal progression of gaps, micromotion, and bone strain was complex and much more variable for post-mortem retrievals compared to the lab prepared specimens. From a clinical perspective, attaining more initial interlock results in cement-bone interfaces that are better fixed with less micromotion.

Correspondence: Kenneth A. Mann, PhD., 3216 Institute for Human Performance, SUNY Upstate Medical University, 750 East Adams Street, Syracuse, New York 13210, 1-315-464-9963 (P), 1-315-464-6638 (F), ; Email: mannk@upstate.edu
MA Miller (millerm@upstate.edu)
JR Goodheart (goodheaj@upstate.edu)
B Khechen (Khechenb@upstate.edu)
KA Mann (mannk@upstate.edu)
D Janssen (Dennis.Janssen@radboudumc.nl)

Contributions: Mark Miller performed specimen preparation, the experimental methods, digital image correlation analysis, and assisted in manuscript preparation. Jacklyn Goodheart contributed to specimen preparation, microCT reconstruction, and solid modeling. Ben Khechen performed digital image correlation strain measurements. Dennis Janssen contributed to experimental design and manuscript preparation. Ken Mann designed experiments, performed statistics, and contributed to manuscript preparation. All authors have read and approved the final submitted manuscript.

Keywords

Trabecular resorption; loosening; knee replacement; micromotion; bone strain; postmortem

Introduction

Total knee replacement (TKR) is the most common total arthroplasty procedure performed in the US. While the procedure is very successful for most patients, aseptic loosening is not uncommon and continues to be the leading cause for revision arthroplasty. Fixation of most tibial components in TKRs is achieved with the use of polymethylmethacrylate (PMMA) cement. The cement interlocks with the trabecular bone bed at the time of surgery and provides initial fixation between the bone and the implant. However, recent postmortem retrieval studies of well fixed joint replacements show that this trabecular interlock with PMMA can resorb with *in vivo* service (1). The trabecular resorption results in weaker fixation at the cement-bone interface (2; 3) and likely contributes to aseptic loosening. This work aims to understand where and how changes to fixation occur with *in vivo* service in functioning joint replacements.

To date, the local micro-mechanical environment of the interlocked cement-trabecular region of TKR, after initial implantation and after *in vivo* service, has not been explored at high resolution and may provide clues as to how the resorption process occurs. The goal of the present study was to quantify the cement-trabeculae micro-morphology and micromechanics for lab prepared specimens (to represent initial post operative state) and *en bloc* postmortem retrievals (that had *in vivo* remodeling) that were not radiographically loose. We asked two research questions: 1) What is the initial state of fixation between trabeculae and cement for the interlocked region in terms of interface gap distribution, interface micromotion, and trabecular bone strain? 2) How does the distribution of gaps, micromotion, and trabecular bone strain change with *in vivo* service?

Methods

Eight postmortem retrieved total knee replacements (TKRs) that were functioning at the time of death (Table 1) were obtained from the SUNY Upstate Anatomical Gift Program (7 female/ 1 male). The knees were disarticulated, tibiae were stripped of soft tissue, and a water irrigated abrasive blade (Isomet 2000, Buehler Inc, Lake Bluff, IL, USA) was used to create sagital and frontal plane cuts through the metal tray, cement and bone. Nine postmortem cement-bone test specimens (two specimens were created from one of the TKRs) with 8×8mm cross-section and 16mm length were created from the underside of the tibial tray, near the center of the medial or lateral tibial plateau (Figure 1A). The specimens had three main regions: a region of interlocked bone between the trabeculae and cement, a cement border that represented the extent of cement penetration into the bone, and the supporting bone that was distal to the cement (Figure 1A). All of the postmortem retrieved knee replacements had metal backed tibial components and were radiographically well-fixed (limited or no radiolucency between cement and bone) based on AP radiograph.

Nine fresh-frozen cadaver knees (Table 1) without implants (7 female/2 male) were used to create the laboratory prepared cement-bone interface specimens. The lab prepared specimens were created to represent the initial state of fixation, prior to any bone remodeling, and were created using conditions that mimicked the intraoperative environment. The proximal tibiae were warmed to 37 deg C in a simulated blood analog solution and were prepared for cementing by creating a transverse cut to accept the tibial component followed by pulsatile lavage. Polymethylmethacrylate (PMMA) cement (Simplex P; Stryker Orthopedics, Mahwah, NJ, USA) was vacuum mixed (Mixevac III, Stryker Orthopedics, Mahwah, NJ, USA) and manually applied to the cut bone surface and was pressed into the trabecular bone bed using spatula and thumb pressurization. A mock metal tray was pressed into place and held until the cement cured. Nine cement-bone specimens (8×8mm cross section, 16mm length) were fabricated for the lab prepared group following the method described above for the postmortem test specimens.

Specimens were cleaned of cutting wear debris using pulsatile lavage and scanned in a micro computed tomography (uCT) scanner at 16 μm isotropic resolution to document the three dimensional morphology of the interlocked trabeculae-cement interface and bone volume fraction (BV/TV) of the supporting bone. Solid model reconstructions were made using MIMICS (Materialise, Plymouth, MI) to visualize the cement-bone interlock.

The specimens were mounted in a custom screw driven loading device that was attached to an x-y machinist's stage (Benchman, Light Machines, Davenport, IA). Prior to imaging, graphite powder was blown onto the specimen surface to increase contrast for subsequent image correlation analysis. Reflected white light images were obtained over the entire 2-D face (Figure 1A) of the test specimen (8×16 mm) at 3.1 μm/pixel `normal' resolution (NR) using a CCD camera (Spot Insight, Diagnostic Instruments, Sterling Heights, MI) attached to a stereo microscope (SMZ800, Nikon Instruments, Melville, NY). This was accomplished by moving the x-y stage in increments to image capture the entire specimen surface, followed by assembly of the image sequence into one large composite image (~ 15 megapixel). The composite image sequence was obtained in the unloaded state, and after an axial compressive loading of 1 MPa was applied. A 1 MPa axial stress was chosen to represent the equivalent of approximately one body weight, non-destructive load, assuming the load is applied uniformly over the tibial tray surface. The NR image data was used to document the global interdigitation and strain in the supporting trabecular bone.

To document gap thickness, micromotion, and axial strain (Figure 1B) of the interlocked trabeculae-cement interface, very high resolution (VHR) (0.5 μm/pixel, 0.8 mm × 0.7 mm field of view) images were captured for the interdigitated cement-bone regions for unloaded and 1 MPa compressive load states. The camera system was moved to new position along the cement-bone interface and the sequence was repeated until all of the interlocked trabeculae-cement areas of the surface were captured.

Fifty random sampling points along the interlocked trabeculae-cement interface of each specimen were selected for gap, micromotion, and trabecular bone strain analysis. The distance from each sampling point within the interlocked region to the cement border (Figure 1A) was determined and was used as a covariate in the data analysis. At each

sampling point, the gap thickness between cement and bone was measured normal to the interface (Figure 1B). Digital image correlation (DIC) (Match ID, Merelbeke, Belgium) was used to determine the relative micromotion due to the 1 MPa load at each sampling point using DIC measurement locations placed on either side of the cement-bone interface. Axial strain in the trabeculae at each sampling point was measured in the direction of the applied load and was calculated using the DIC relative displacements over a 300 μm gage length. The supporting bone strain was calculated using the DIC relative displacement between the distal end of the bone and proximal end of the bone with NR image sets. Preliminary studies were used to assess the accuracy of the DIC system using a calibration system using NR and VHR image modes. For a 5.00 μm known excursion (micromotion) in NR mode, there was a 0.08 μm root mean square error (RMSE) in excursion measurement. For a known excursion of 1.00 μm in VHR mode, the RMSE was 0.06 μm.

Documenting Trabecular Resorption

The initial state of fixation for the postmortem retrievals can be inferred from the shape of the cement layer that interlocked with the trabecular bone at the time of surgery (1). The doughy cement that is pressed into the trabecular bone bed cures in place in a form that corresponds to the trabecular bone (Figure 2A). After trabecular resorption (Figure 2B–D), cavities are left in the cement layer, indicating regions where trabeculae had originally existed. To characterize the state of interlock between trabeculae and cement, the initial and current interdigitation depths were calculated. The initial cement-bone interdigitation depth (inID) was calculated as the average distance between a line that followed the initial extent of penetration of trabeculae into the cement and the cement border. The current interdigitation depth (curID) was calculated as the average distance between a line that followed the current extent of trabeculae into the cement layer and the cement border. A previous repeatability study (1) found that standard error of the mean was 7.0 and 4.0 μm for inID and curID measurements, respectively.

Statistical Analysis

Descriptive statistics were calculated for the donor data and the mechanics/morphology metrics of the interlocked and supporting trabecular bone. Gap thickness, trabeculae-cement micromotion, and trabecular bone strain served as the primary dependent variables in this study. Linear regression analysis was used to determine if the dependent variables (gap thickness, micromotion, strain) decreased with distance from the cement border for the lab prepared specimens. A paired t-test was used to determine if the interdigitated trabecular bone strain was different from the supporting bone strain. Analysis of covariance (ANCOVA) was used to determine if the gap thickness, micromotion, and bone strain was different for the lab prepared and postmortem specimens using distance from the cement border as a covariate.

Results

The postmortem (PM) and lab prepared (LP) specimens had similar characteristics (Table 1) in terms of donor age (average PM/LP: 73/77 years), supporting bone volume fraction (BV/TV average PM/LP: 0.115/0.122), and initial interdigitation depth (inID PM/LP:

1.7/2.3 mm). The supporting bone strain when loaded with 1 MPa compression (PM/LP: −2030/−1320 με) was on average higher for the postmortem retrievals, but there was not a statistically significant difference between groups (p=0.22). The range of supporting bone strains for the postmortem retrievals (−90 to −4820 με) was larger than the lab prepared bone strains (−520 to −2020 με). With *in vivo* service (ave 6.5 years, range 1 to 16), there was loss of cement-bone interlock (Figure 2), but the amount of loss was quite variable. One donor, a 61-year-old male with 5 years in service had only limited resorption with continued extensive interlock between cement and bone (Figure 2B). In contrast, an 87-year-old female, with three years in service, had extensive trabecular resorption (Figure 2C) with evidence of some residual bone left deep in the cement layer. A 69-year-old female with 11 years in service showed extensive resorption (Figure 2D) with very little bone remaining in the cement layer and limited points of contact between the cement and supporting trabecular bone.

For the lab prepared specimens, there was a gap between trabeculae and cement with an average thickness of 14 μm (Table 1) and this was not dependent on the distance from the cement border (r^2=0.048, p=0.139) as tested using linear regression. Trabeculae-cement micromotion was very small (mean: 1.03 μm) and was higher near the cement border compared to deep in the cement layer (r^2=0.16, p=0.0059). Trabecular bone strain in the interdigitated region (mean: −410 με) was also higher near the cement border compared to deep in the cement layer (r^2=0.16, p=0.0057). To bone exclude strain measurements nearest the cement layer that were not truly interlocked with cement, we investigated a subset of interlocked bone strain results that were more than 0.25mm from the cement border. The interdigitated bone strain for locations more than 0.25mm from the cement border (mean: −270 με) was five times smaller than the supporting bone strain in the lab prepared specimens (mean: −1320 με). This difference was statistically significant (p=0.0002) using a paired t-test.

The distribution of gaps between trabeculae and cement as a function of distance from the cement border for the 9 postmortem retrieval specimens is shown in Figure 3A. The results are `binned' into 0.5 mm groups and the median value for each bin is plotted. The average gap distribution of the 9 lab prepared specimens is also shown. For each specimen, the average initial interdigitation depth (inID), maximum inID, and years in service are listed. Some postmortem retrieval specimens have gap distribution patterns similar to the lab prepared specimens (e.g. specimen indicated by `b' in Figure 3A with inID=2.9mm at 5 years in service; specimen also shown in Figure 2B), although the gaps appear to be somewhat larger near the cement border. Other retrieval specimens show larger gaps near the cement border and small gaps for trabeculae left deep in the cement layer (e.g. `c' with inID=2.6mm at 3 years in service). Specimens with very little remaining interlock often have larger gaps near the cement border (e.g. `d' with inID=1.7mm at 11 years in service). As a group (Figure 4A), gaps are larger for the postmortem retrievals (average PM/LP = 40/14 μm), are larger near the cement border, and the relationship between gap size and distance from the cement border is different for lab prepared and postmortem retrievals (p=0.0079) (ANCOVA statistics shown in Table 2).

The pattern of trabeculae-cement micromotion (Figure 3B) generally follows that of trabeculae-cement gap thickness. The specimens with substantial remaining interlock exhibit very small micromotion (< 1 μm), while those with substantial trabecular resorption have greater micromotion (> 10 μm) near the cement border. As a group (Figure 4B), trabeculae-cement micromotions are larger for the postmortem retrievals (average PM/LP = 5.7/1.0 μm), are larger near the cement border, and the relationship between micromotion and distance from the cement border is different for lab prepared and postmortem retrievals ($p=0.0003$) (ANCOVA statistics shown in Table 2). Specimens with more time in service ($p=0.0006$) and less initial interdigitation ($p=0.031$) had more micromotion ($r^2=0.73$), tested using multiple regression.

In contrast to gap thickness and micromotion, the axial bone strains for trabeculae that interlock with cement (Figure 3C) were not different between the postmortem and lab prepared groups (average PM/LP: −1380/−410 με, $p=0.81$) (Figure 4C, ANCOVA in Table 2). However, both groups did show a decrease in trabecular bone strain with increasing distance from the cement border ($p=0.006$). Also of note was the large variability in strain magnitudes for data collected near the cement border for the postmortem retrievals. Some specimens, particularly those with substantial remaining interlock, had very low interdigitated bone strains. In contrast, retrieval specimens with very little remaining interlock, had high compressive strains (~−4000 με). The interlocked trabecular bone strain for the postmortem retrievals was lower than the supporting bone strains ($p=0.0148$).

Discussion

The results from this study show that the trabeculae that initially interlock with PMMA cement in knee replacements are not in direct apposition; small gaps exist over much of the interface between cement and bone. When loaded, there is a small amount of micromotion between the trabeculae and cement, with a greater degree of micromotion near the cement border compared to deep within the cement layer. With *in vivo* service, local trabecular resorption causes gaps between the trabeculae and cement surface to become much larger. The larger gaps allow for more micromotion near the cement border. For some cases, in which there is extensive trabecular resorption, the trabecular bone remaining deep in the cement layer can have small gaps and negligible micromotion. In some instances, this bone is no longer physically connected to the supporting trabecular bone and likely does not play an important role in load transfer between the trabecular bone and cement.

Trabecular bone strain measured in the interlocked region for the lab prepared specimens was on average 20% of the apparent strain of the supporting bone that was not interdigitated with cement. It should be noted that the axial strain measured in the interdigitated region was measured using a gage length of 300 μm, while that apparent strain in the supporting bone was measured over the vertical length of the bone (~10–15mm). As such, the reported interlocked trabecular strain was consistent with a tissue strain measure, while the supporting bone strain was an apparent strain measure. Finite element modeling has been used previously to relate tissue strain within trabecular bone to the global applied apparent strain. For models of human vertebral bone, Morgan et al (4) found median minimum principal strains of −2500 με for a compressive apparent strain of −4500 με, giving a

tissue:apparent strain ratio of 0.55. Nagaraja et al (5) calculated −2500 με minimum principal tissue strain for −7500 με applied apparent strain using bovine proximal tibia bone, resulting in a tissue:apparent strain ratio of 0.35. Finally, Harrison et al (6) calculated −1000 με minimum principal tissue strain for −1000 με applied apparent strain using for an ovine vertebrae, giving a 1.0 tissue:apparent strain ratio. The lower tissue:apparent strain ratio in the current study (axial interdigitated bone strain/supporting bone strain = −270/−1320 με = ~ 0.2) suggests that the trabeculae interlocked with cement are strain shielded because the tissue strains are much lower than cases reported for normal bone without PMMA cement. Further clarification of the magnitude of strain shielding would best be performed with a finite element model in which the appropriate interface characteristics are included between the trabeculae and cement.

The mechanics of interdigitated cement-bone constructs has recently been studied in the context of understanding damage mechanisms to the cement and bone during loading (7) using digital volume correlation and finite element modeling. For a case in which there was a BV/TV in the range used in this study (0.14), failure localized to the supporting bone through bending and buckling of the trabeculae adjacent to the cement layer. While modeling was performed with a frictional interface between cement and trabecular bone, the micromotion and strain shielding of trabeculae in the interlocked region was not explored.

Evidence of small gaps between trabeculae and cement has been reported for cement augmentation (8; 9) used to treat or prevent vertebral collapse (vertebroplasty and kyphoplasty). In those studies, finite element modeling of the composite cement-bone constructs also showed that use of a frictional interface could more accurately simulate the mechanics of the composite structures compared to one that considered the interface to be bonded. These findings are consistent with the current study suggesting that small gaps form during the flow and curing of PMMA cement around trabeculae and there is not a bond between the components. This would allow for micromotion when loaded.

The most important limitation of this study was that all measurements were made on the specimen surface. Specimen sectioning could alter load transfer through the structure and locally increase or decrease micromotion or strain measurements. Finite element analysis of the full specimen including bone-cement gaps, could be used to compare surface and internal micromotion and strain measurements, thereby determining the effect of sectioning on alteration of the local micromechanics. Pilot FE work of a lab prepared specimen showed that the median micromotion measured at the surface of the specimen (0.303 μm) was slightly larger (11%) than microcromotion measured in the internal regions of the specimen (0.273 μm). It is important to note that the extensive trabecular resorption that occurs with *in vivo* service may have a more important effect on load transfer compared to a sectioning artifact, as was evident in the large variation of results from the postmortem retrievals. An additional limitation is that only one loading condition was considered (axial compression). In-plane shear, out of plane shear, and tension could all occur during physiologic loading. However, axial compression is by far the largest component of loading under the tibial tray (10). The specimens used from each donor are only representative of the interface fixation under the tibial tray for that particular donor. Different regions under the tray will have different amounts of initial interdigitation depth, current interdigitation, and quantity of

supporting bone. Finally, there was an assumption that each specimen would experience 1 MPa of compression during loading, but it is likely that load transfer is not uniform under the tray and some regions would see more and some less applied stress during functional loading.

The mechanism or mechanisms that cause resorption of trabecular bone that initially is interlocked with PMMA cement is not clear. It appears that trabecular resorption may first occur closer to the cement border, compared to deep in the cement layer, based on observation of the resorption patterns in which trabeculae are sometimes left deep in the cement layer. Further work is needed to characterize the pattern of resorption using a larger series of retrievals. Bone closer to the cement border region would have direct access to adjacent bone marrow containing hematopoietic stem cells that could give rise to osteoclastic bone resorption. But the trigger for what would appear to be osteoclastic bone resorption is not clear. Strain shielding of trabecular bone that interlocked with the cement as found in this study could initiate a local resorption process. Pumping of fluid along the thin gaps of the trabeculae-cement interface could cause high local shear stresses and pressure and result in fluid induced osteolysis (11; 12). Polyethylene (PE) wear debris from the articulating surface could also migrate along the interface and initiate focal osteolysis. PE wear particles have not been directly observed at the cement-bone interface for functioning joint replacements, but has been measured in the synovial fluid of TKR (13) and in periprosthetic tissues of loose TKRs (14). It should be noted that there was not evidence of lytic lesions in the bone surrounding any of the postmortem retrievals tested in this study. Thermal necrosis (15) or monomer toxicity (16) could also contribute to bone loss.

It is important to note that trabecular resorption does not consistently occur in all *in vivo* cases. The postmortmen retrievals exhibited a wide range of interlock morphology and micromechanics, and this variation may depend on donor sex, age, and time in service. The least resorption and micromotion occurred in a relatively young 61-year-old male with 5 years of *in vivo* service, suggesting that robust interlock at the interface can be maintained, at least in the short term. In contrast, the two donors with extensive resorption and the most micromotion were female, 69 and 75-years-old, with 11 and 16 years of *in vivo* service. Because micromotion is clearly related to the amount of interlock remaining between cement and bone, interventions that aim to maintain trabecular interlock could improve the long-term outcome for patients with TKRs.

This work shows that the local trabeculae-cement morphology affects interlock micromotion and bone strain. For postmortem retrievals where there was less initial interlock and more time in service, there was more micromotion between the remaining interlocked trabeculae and cement. This is consistent with a previous study where we quantified the global micromotion for transverse sections of postmortem retrieved tibial components; implant sections with greater initial interlock had less micromotion after *in vivo* service (17). From a clinical perspective, attaining more initial interlock appears to result in cement-bone interfaces that are better fixed with less micromotion. This would seem desirable from the perspective of minimize pumping of fluid or debris along the interface (18) and maintaining interface strength (2).

Acknowledgements

The research reported in this publication was supported by the National Institute of Arthritis and Musculoskeletal and Skin Diseases of the National Institutes of Health under Award Number AR42017. The content is solely the responsibility of the authors and does not necessarily represent the official views of the National Institutes of Health. The authors would like to acknowledge the assistance of Dan Jaeger for providing the postmortem retrievals and tissue from the SUNY Upstate Anatomical Gift Program.

REFERENCES

1. Miller MA, Goodheart JR, Izant TH, et al. Loss of Cement-bone Interlock in Retrieved Tibial Components from Total Knee Arthroplasties. Clin Orthop Relat Res. 2014; 472:304–313. [PubMed: 23975251]
2. Goodheart JR, Miller MA, Mann KA. In vivo loss of cement-bone interlock reduces fixation strength in total knee arthroplasties. J Orthop Res. 2014; 32:1052–1060. [PubMed: 24777486]
3. Gebert de Uhlenbrock A, Puschel V, Puschel K, et al. Influence of time in-situ and implant type on fixation strength of cemented tibial trays - a post mortem retrieval analysis. Clin Biomech (Bristol, Avon). 2012; 27:929–935.
4. Morgan EF, Yeh OC, Keaveny TM. Damage in trabecular bone at small strains. Eur J Morphol. 2005; 42:13–21. [PubMed: 16123020]
5. Nagaraja S, Couse TL, Guldberg RE. Trabecular bone microdamage and microstructural stresses under uniaxial compression. J Biomech. 2005; 38:707–716. [PubMed: 15713291]
6. Harrison NM, McHugh PE. Comparison of trabecular bone behavior in core and whole bone samples using high-resolution modeling of a vertebral body. Biomech Model Mechanobiol. 2010; 9:469–480. [PubMed: 20066462]
7. Tozzi G, Zhang QH, Tong J. Microdamage assessment of bone-cement interfaces under monotonic and cyclic compression. J Biomech. 2014; 47:3466–3474. [PubMed: 25283468]
8. Kinzl M, Boger A, Zysset PK, Pahr DH. The mechanical behavior of PMMA/bone specimens extracted from augmented vertebrae: a numerical study of interface properties, PMMA shrinkage and trabecular bone damage. J Biomech. 2012; 45:1478–1484. [PubMed: 22386105]
9. Helgason B, Stirnimann P, Widmer R, Ferguson SJ. Experimental and computational models to investigate the effect of adhesion on the mechanical properties of bone-cement composites. J Biomed Mater Res B Appl Biomater. 2011; 99:191–198. [PubMed: 21714083]
10. Kutzner I, Heinlein B, Graichen F, et al. Loading of the knee joint during activities of daily living measured in vivo in five subjects. J Biomech. 2010; 43:2164–2173. [PubMed: 20537336]
11. Fahlgren A, Bostrom MP, Yang X, et al. Fluid pressure and flow as a cause of bone resorption. Acta Orthop. 2010; 81:508–516. [PubMed: 20718695]
12. Mann KA, Miller MA. Fluid-structure interactions in micro-interlocked regions of the cement-bone interface. Comput Methods Biomech Biomed Engin. 2014; 17:1809–1820. [PubMed: 23480611]
13. Minoda Y, Kobayashi A, Iwaki H, et al. Polyethylene wear particles in synovial fluid after total knee arthroplasty. Clin Orthop Relat Res. 2003:165–172. [PubMed: 12771827]
14. Schmalzried TP, Jasty M, Rosenberg A, Harris WH. Polyethylene wear debris and tissue reactions in knee as compared to hip replacement prostheses. J Appl Biomater. 1994; 5:185–190. [PubMed: 10147443]
15. Stanczyk M, van Rietbergen B. Thermal analysis of bone cement polymerisation at the cement-bone interface. J Biomech. 2004; 37:1803–1810. [PubMed: 15519587]
16. Gough JE, Downes S. Osteoblast cell death on methacrylate polymers involves apoptosis. J Biomed Mater Res. 2001; 57:497–505. [PubMed: 11553879]
17. Miller MA, Terbush MJ, Goodheart JR, et al. Increased initial cement-bone interlock correlates with reduced total knee arthroplasty micro-motion following in vivo service. J Biomech. 2014; 47:2460–2466. [PubMed: 24795171]
18. Bostrom M, O'Keefe R. What experimental approaches (eg, in vivo, in vitro, tissue retrieval) are effective in investigating the biologic effects of particles? J Am Acad Orthop Surg. 2008; 16(Suppl 1):S63–67. [PubMed: 18612016]

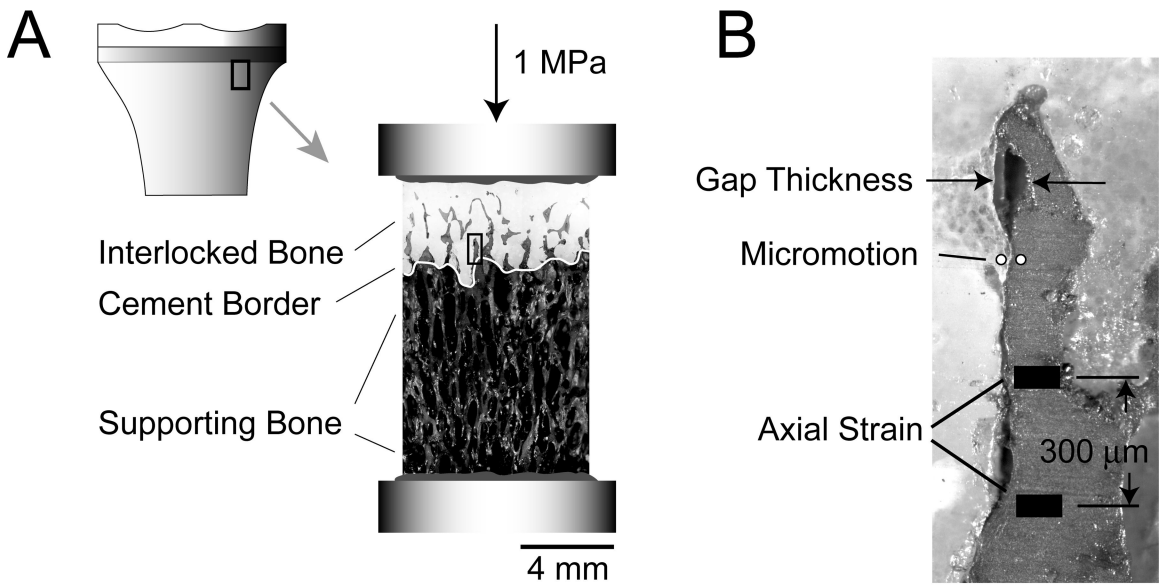

Figure 1.

Small segments of the cement-bone interface from below the tibial tray were sectioned (**A**) and loaded in axial compression to 1 MPa. The gap thickness, micromotion, and axial strain were measured at 50 randomly selected points along the trabeculae-cement interface (**B**). The gap thickness and micromotion measures were made across the trabeculae-cement interface. The axial bone strain was measured across a 300 μm gage length in the axial direction. All three measurements were made at coincident sampling points along the interface; they are shown here at three distinct locations for clarification purposes. The selected image in panel B is taken from the region of interest indicated by the black rectangle in the center image.

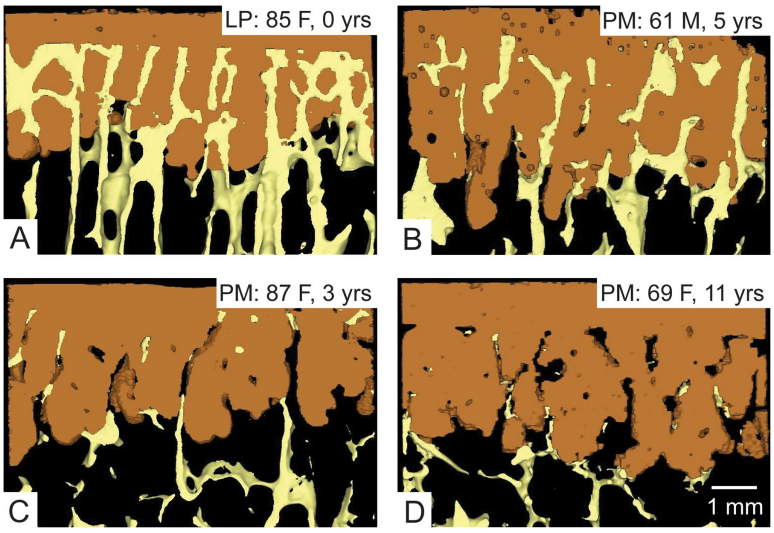

Figure 2.

Micro computed tomography (uCT) reconstructions of the interlocked cement-bone interface illustrating a range of interlock conditions. A laboratory prepared (LP) specimen (**A**) has no resorption, while postmortem retrieval (PM) specimens show limited (**B**), extensive (**C**), and near complete (**D**) resorption of trabeculae from the interlocked cement layer. Donor age, sex, and years in service are shown.

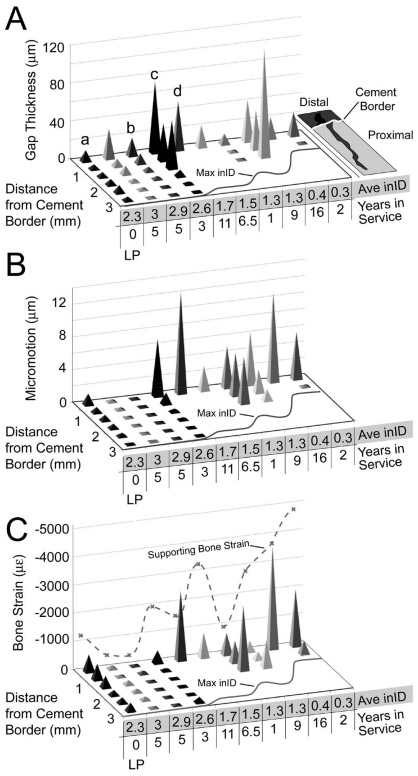

Figure 3.

Median trabeculae-cement gap (**A**), micromotion (**B**), and trabecular bone strain (**C**) as a function of distance from the cement border for the 9 postmortem retrieval specimens and the average of the 9 laboratory prepared (LP) specimens. The average initial interidigitation (inID) and years in service are shown. The maximum initial interdigitation (Max inID) is shown graphically along the base of the plots and the supporting bone strain is shown as a dashed line along the vertical axis. Data are divided into 0.5 mm bins for each specimen. The lower case a, b, c, d indicated in panel A correspond to panels A-D in Figure 2.

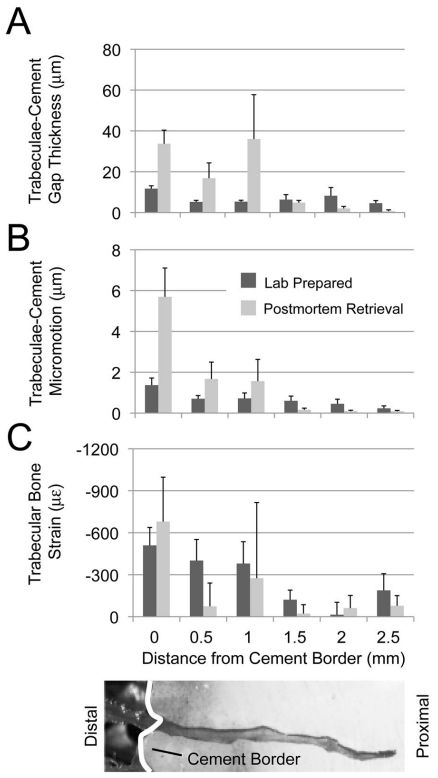

Figure 4.

Mean and standard error magnitudes for trabeculae-cement gap thickness (**A**), micromotion (**B**), and trabecular bone strain (**C**) for the lab prepared and postmortem retrieval groups. Data are divided into 0.5 mm bins for each group.

Table 1

Summary characteristics of the 18 test specimens from lab prepared (9 LP, n=9 donors) and postmortem retrieval TKRs (9 PM specimens from n=7 donors, 1 donor had bilateral implants, 2 specimens from one donor).

Donor Data	**Type**	**Mean**	**Standard Dev**	**Min**	**Max**
Age (years)	LP	76.7	8.7	64	90
	PM	72.9	8.7	61	87
Weight (kg)	LP	90.1	18.0	65	117
	PM	78.3	17.7	61	103
Time in service (years)	LP	0	0	0	0
	PM	6.5	4.8	1	16
Supporting Bone Morphology & Mechanics					
Supporting bone fraction (BV/TV)	LP	0.122	0.054	0.072	0.236
	PM	0.115	0.042	0.065	0.173
Supporting bone strain (με)	LP	−1320	545	−2020	−520
	PM	−2030	1570	−4820	−90
Interlock Morphology					
Initial interdigitation depth, inID (mm)	LP	2.3	0.7	1	3.2
	PM	1.7	1	0.3	3.0
Current interdigitation depth, curID (mm)	LP	2.3	0.7	1	3.2
	PM	1.1	1.2	0	3.0
Gap thickness (μm)	LP	14.0	4.1	7.1	21.2
	PM	40.5	17.8	14.1	60.3
Interlock Mechanics					
Trabeculae-cement micromotion (μm)	LP	1.03	0.61	0.22	2.17
	PM	5.67	4.71	0.1	13.1
Interdigitated trabecular bone strain (με)	LP	−410	330	−1060	−16
	PM	−1380	1530	−4300	15
Interdigitated trabecular bone strain (με) with distance from cement border > 0.25 mm	LP	−270	290	−830	52
	PM	−66	370	−500	550

Table 2

Analysis of Covariance (ANCOVA) results for the gap thickness, micromotion, and bone strain as a function of interface type (lab prepared/postmortem), distance from the cement border, and the interaction term (Type * Distance).

Parameter	Gap Thickness	Micromotion	Bone Strain
Type (LP/PM)	0.0009	0.001	0.81
Distance from Cement Border	0.001	0.0001	0.006
Type * Distance (slope)	0.0079	0.0003	0.72